PAPER

Ultrafast time delay as a control parameter in resonant ionization by two XUV ultrashort pulses

IOP Publishing Journal of Physics B: Atomic, Molecular and Optical Physics
J. Phys. B: At. Mol. Opt. Phys. **53** (2020) 095603 (9pp) https://doi.org/10.1088/1361-6455/ab787b

Ultrafast time delay as a control parameter in resonant ionization by two XUV ultrashort pulses

Theodoros Mercouris[1], **Yannis Komninos and Cleanthes A Nicolaides**

Theoretical and Physical Chemistry Institute, National Hellenic Research Foundation, 48 VasileosConstantinou Avenue, Athens 11635, Greece

E-mail: thmerc@eie.gr, ykomn@eie.gr and caan@eie.gr

Received 23 September 2019, revised 11 February 2020
Accepted for publication 20 February 2020
Published 3 April 2020

Abstract

We predict quantitatively that it is possible to use few-femtosecond positive or negative *time delays*, Δt, between two XUV Gaussian few-femtosecond pulses of moderate intensities and central frequencies ω_1 and ω_2, in order to control the probability of ionization at clearly defined exit energies corresponding to the sums of photon frequencies $(\omega_1 + \omega_1)$, $(\omega_2 + \omega_2)$, and $(\omega_1 + \omega_2$, or $\omega_2 + \omega_1)$. The phenomenon is demonstrated quantitatively by obtaining and using nonperturbative solutions of the time-dependent Schrödinger equation for a time-dependent scheme involving the process of two-photon resonant ionization of Helium via the $1s2p\ ^1P^o$ (58.4 nm) and $1s4p\ ^1P^o$ (52.22 nm) excited states. The calculations used wavefunctions which are *state-specific* for the discrete spectrum, (up to the $1s7g\ ^1G$ Rydberg state), as well as for the energy-normalized continuous spectrum, (up to 2.0 a.u. above threshold with angular momenta $\ell = 0, 1, 2, 3, 4$). For this system, using Δt as a control knob, the effects on the photoelectron spectrum of the combination of the transition amplitudes via the two paths and their interference are determined clearly for pulses with field-cycles ranging from about 15 to about 80 cycles. The analysis has included the comparison of the nonperturbative results, obtained by implementing the *state-specific expansion approach*, with those obtained from the application of second order time-dependent perturbation theory with two Gaussian pulses of finite duration.

Keywords: atomic processes in external fields, ultrafast time delay control, multiphoton ionization

1. Time delay as a control parameter in a two-photon resonant ionization process with two XUV ultrashort pulses

Current experimental/technological work in many facilities by large teams around the world aims at improving the performance and versatility of sources of radiation pulses that can produce ultrashort pulses at different ranges of wavelengths, having weak, moderate or strong intensities, say between 10^{11} and 10^{14} W cm^{-2}. This work involves the production and application of either table-top, high-harmonic generation (HHG)-based pulses, or, of well-characterized pulses from free-electron laser (FEL), whose duration is in the range of a few decades of femtosecond (fs) down to decades of attosecond (*as*). In principle, such pulses are suitable for use in a variety of new types of spectroscopic studies in atomic, molecular and optical (AMO) physics.

These developments, in conjunction with corresponding advances of theory and of many-electron methods that can deal quantitatively with the solution of the many-electron time-dependent Schrödinger equation (METDSE) and with its appropriate utilization, have ushered AMO physics into a new era of spectroscopy, where the physically relevant information about electron dynamics with respect to ultrashort

[1] Author to whom any correspondence should be addressed.

changes of time can be understood not only phenomenologically or descriptively, but even quantitatively for real systems.

Brief discussions on aspects of the progress that has thus far been achieved experimentally and on prospects for applications to various problems and areas of physics and chemistry using such pulses and corresponding spectroscopic techniques, were recently presented in this Journal, in a compendium of short articles by many authors in [1]. The generation and application of well-characterized FEL pulses of short wavelengths, say in the extreme ultraviolet (XUV) and beyond, is expected to open new vistas in the study of time-resolved electron dynamics.

Of recent interest to us [2] was the quantitative study and analysis of the *absolute cross-sections* of the two-XUV photon ionization of Helium, on-and off-resonance with the Rydberg states $1s2p\ ^1P^o$, $1s3p\ ^1P^o$ and $1s4p\ ^1P^o$, which were obtained by averaging the time-dependent probabilities that emerged from the nonperturbative solution of the METDSE. The impetus for that study came from the publication of the first measurements of these quantities using XUV pulses from the FEL in RIKEN, Japan [3, 4]. Among other things, the experimental work of Fushitani *et al* [4] included the investigation of aspects of the spectroscopy which is possible when two-color fs pulses, with time delay Δt, are used for the study of the ionization of Helium. They combined an ultrashort optical laser pulse of 268 nm (4.63 eV) with FEL pulses of 59.7 nm (20.8 eV). The results of [2] were compared with the experimental values and with earlier theoretical results from perturbative as well as nonperturbative time-independent calculations. For the conclusions the reader is referred to [2].

In view of the developments discussed in [1–4] and in their references, a question which is relevant to time-resolved electron dynamics is the following:

What kind of new information can be extracted when, instead of one, two ultrashort pulses with XUV or shorter wavelengths are generated and used in time-dependent spectroscopy with atoms or with their positive ions ? For example, in a recent publication co-authored by 40 scientists, Prince *et al* [5] reported experimental results on the *coherent control* [6] of an ionization process in Neon at the level of only a few *as* time-resolution, using two XUV (63.0 and 31.5 nm) fs pulses and adjusting their *phase difference*, φ, so as to control the asymmetry of the photoelectron angular distribution. The authors of [5] argued that their experimental demonstration '*opens the door to new short-wavelength coherent control experiments with ultrahigh time resolution and chemical sensitivity*', (abstract of [5]), with prospects of new types of application, '*in analogy to what happened in the last few decades in the field of optical laser-based research*'. (Prince and Masciovecchio, on page 16 of [1]).

The theoretical work reported here has taken our earlier investigations [2] to a more complex and challenging level, by exploring quantitatively the possibility of *control* of a two-photon resonant ionization process in Helium, when two different, time-delayed XUV pulses with ultrashort duration are used.

In the early, optical laser-based research on processes of photodissociation and of photoionization, the underlying principle is the presence of *interference* of different excitation paths ending at the same final state in the continuum, where the control knob is the *relative phase* [6]. Extensions and time-independent many-electron computational implementations to ionization dynamics which determine the functional dependence (sinusoidal) of the '*interference generalized cross-section*' on the *phase differences* between dichromatic or trichromatic weak AC fields can be found in [7]. We note that the use of the relative phase as a control parameter in two-color studies of spectroscopy where interference plays a crucial role, continues to find new areas of application, e.g. [8].

In the present work, we examine a different possibility, where the understanding of the phenomenon requires the calculation and use of time-dependent solutions of the METDSE that account for the interplay between electronic structures, state-mixings, spectral features and time-dependent ionization dynamics. The problem involves the study from first principles of the effects on the *two-photon resonant* photoelectron spectrum of the combination of the transition probabilities via two paths and their interference, as a function of the *time-delay*, Δt, between the applied ultrashort pulses.

The chosen physical system is that of Helium irradiated by two XUV ultrashort Gaussian pulses of moderate intensities, 1×10^{12} W cm^{-2} and 8×10^{12} W cm^{-2}, which are applied with negative (the ω_2 pulse precedes the ω_1 pulse) or positive time delay, Δt, and whose wavelengths are chosen so as to cause two-photon resonant ionization through the transitions $1s^2\ ^1S_0 \rightarrow 1s2p\ ^1P_1^o$ at 58.4 nm and $1s^2\ ^1S_0 \rightarrow 1s4p\ ^1P_1^o$ at 52.22 nm.

In lowest order, the excitation scheme is written as

$$\text{He}\quad 1s^2 \xrightarrow{\omega_1} 1s2p \xrightarrow{\omega_2} 1s(\varepsilon s\ or\ \varepsilon d)\quad \text{and,}\quad 1s^2 \xrightarrow{\omega_2} 1s4p \xrightarrow{\omega_1} 1s(\varepsilon s\ or\ \varepsilon d),\ \text{(A)}$$

$\omega_1 = 0.78$ a.u. and $\omega_2 = 0.87$ a.u. are the central frequencies of the two pulses. The same final scattering state is reached via the two paths, while interference can occur.

The question which we asked and answered in this work quantitatively is the following: To what degree does the ionization probability depend on the variation of Δt from relatively large positive to relatively large negative values, as the system is excited via the two paths and their interference?

We note that, in the previous era of optical lasers and AC fields, the importance of interference on the time-independent rate of two-photon transitions to the continuum was first proposed by Chen, Shapiro and Brumer [6, 9] and was first demonstrated experimentally by Pratt [10], followed by Wang and Elliott [11]. Their analysis was based on the time-independent formula of lowest order perturbation theory and on consideration of quantities such as the degree of detuning, laser power, or relative polarization, as control parameters [10, 11].

In the present case of ultrashort, time-delayed XUV pulses, the theoretical treatment must necessarily involve time

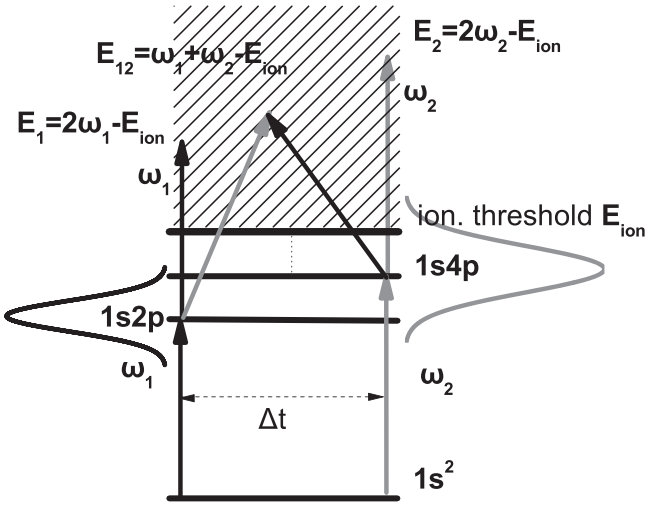

Figure 1. The scheme in the two- XUV photon resonant ionization of Helium chosen for the present study of the possibility of using the ultrashort *time delay*, Δt, between the instants of application of the two ultrashort Gaussian XUV pulses, as a control knob. For the $1s2p\ ^1P^o$ state, $\omega_1 = 0.78$ a.u. (58.4 nm), and for the $1s4p\ ^1P^o$ state, $\omega_2 = 0.87$ a.u. (52.2 nm). The pulse durations are of the order of a few femtoseconds. The black and gray curves surrounding the two discrete levels represent realistically the energy profiles of the pulses, with central frequencies ω_1 and ω_2.

explicitly, apart from having to compute N-electron matrix elements. The relevant information is obtained from systematic calculations that solve the METDSE nonperturbatively, using a two-color perturbation $\boldsymbol{V}_{\rm int}(t) = \boldsymbol{V}_1(\omega_1, t) + \boldsymbol{V}_2(\omega_2, t + \Delta t)$. Now, it is Δt that has the role of the control knob. In addition, results were obtained by applying second order time-dependent perturbation theory, (SOTDPT), with explicit incorporation of the characteristics of the two pulses.

2. Construction of the problem and quantitative solution

The proposal of the two-photon resonant ionization of Helium using two ultrashort XUV pulses which was outlined in the Introduction, is displayed in figure 1. The main goal was to identify quantitatively, from first principles, a set of parameters of two XUV Gaussian pulses and the corresponding values of ultrashort time delays, Δt, that can be used to affect in a significant and controllable way the photoelectron spectrum. As discussed in section 3, this has proven possible. The duration of either pulse is in the range of a few femtoseconds, for intensities in the range 1×10^{12}–1×10^{13} W cm^{-2}. Time-consuming nonperturbative calculations also showed that, for intensities close to 10^{14} W cm^{-2}, the resulting spectrum loses its clarity, indicating the presence of strong shifting and mixing of states and transition amplitudes from both the discrete and the continuous spectrum.

The photoelectron peak around the energy $E_{12} = \omega_1 + \omega_2 - E_{\rm ion}$, is essentially independent of the phase difference, φ, because the two paths reaching E_{12} have the same dependence on it. This is a convenient condition for experimentalists, because the steady control of φ for FEL pulses of high energy is not achievable easily.

On the other hand, we expect that Δt should play a significant role in the vicinity of E_{12}, because, for ultrashort pulses, the population transfer to the intermediate states $1s2p\ ^1P^o$ and $1s4p\ ^1P^o$ is strongly dependent on it. It follows that the magnitudes of the photoelectron peaks corresponding to the photon frequencies $(\omega_1 + \omega_1)$, $(\omega_2 + \omega_2)$, and $(\omega_1 + \omega_2$, or $\omega_2 + \omega_1)$, will also depend on Δt and, of course, on intensity, in a way which cannot be predicted without accurate calculations that solve the METDSE with a two-color time-dependent interaction operator, $\boldsymbol{V}_{\rm int}(t)$.

The basic step towards the quantitative understanding of the electron dynamics associated with the processes of figure 1 is the calculation of the solution of the METDSE from first principles. This was done nonperturbatively by implementing the *state-specific expansion approach* (SSEA) [12]. For reasons of comparison and for additional insight into the role of the continuum and of discrete states other than the $1s2p\ ^1P^o$ and the $1s4p\ ^1P^o$, the METDSE was also solved at the level of SOTDPT with Gaussian pulses of finite duration —see below.

The fundamental equations are

$$\boldsymbol{H}(t)\Psi(t) = i\hbar\frac{\partial\Psi(t)}{\partial t}, \tag{1a}$$

$$\begin{aligned}\boldsymbol{H}(t) &= \mathbf{H}_{atom} + \boldsymbol{V}_{\rm int}(t),\\ \boldsymbol{V}_{\rm int}(t) &= \boldsymbol{V}_1(\omega_1, t) + \boldsymbol{V}_2(\omega_2, t + \Delta t).\end{aligned} \tag{1b}$$

In our work, the coupling operator in $\boldsymbol{V}_{\rm int}(t)$ is the full multipolar electric Hamiltonian, H_{el}

$$H_{el} = e\sum_j \int_0^1 \vec{r}_j \cdot \vec{E}(\lambda\vec{\kappa}\cdot\vec{r}_j)d\lambda. \tag{2}$$

The compact form (2) is taken from equation (5.35) of Loudon's book [13]. The reasons for choosing (2) and the theory which deals with the properties of this operator when calculating *bound-bound*, *bound-free* and *free-free* matrix elements in spherical symmetry, can be found in [14] and its references.

As we have argued in the past [12, 14], of special significance in the general problem associated with the systematic nonperturbative solution of the METDSE for field-induced electron dynamics, is the correct and systematic calculation of the on- and the off-resonance *free-free* (continuum-continuum) matrix elements. When the state-specific, energy-normalized, proper scattering wavefunctions are employed, these matrix elements are characterized by *singularities* on the energy axis. Taking account of them, in a rigorous and numerically accurate way, is essential for securing the reliability of nonperturbative solutions of the METDSE, especially since in the general many-electron, many-channel problem, their number is huge. We have shown [14], that when, instead of the unbounded electric dipole operator $\boldsymbol{r}$, the operator of equation (2) is used in the calculation of the required matrix elements with the electric dipole selection

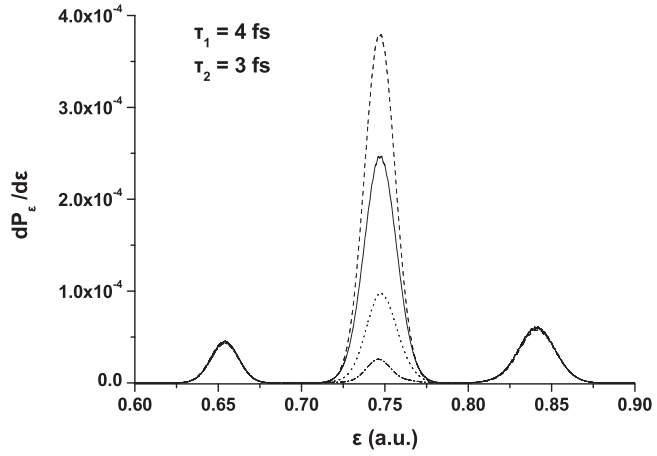

Figure 2. Photoelectron spectrum for the two-XUV photon resonant ionization of Helium according to the scheme of figure 1. $\frac{dP_\varepsilon}{d\varepsilon}$ is the probability distribution per atomic unit of energy, defined and computed by equation (5). The full widths at half maximum, τ_1 and τ_2, are of the order of 20 cycles of each field. The curves correspond to positive and negative values of time delay, Δt. The solid line curve corresponds to $\Delta t = 0$ fs, the dashed one to $\Delta t = 2.4$ fs, the dotted one to $\Delta t = -2.4$ fs, and the dashed–dotted one to $\Delta t = -4.8$ fs. The left and right peaks represent the two-photon ionization of He ionization, with $\omega_1 = 0.78$ a.u. (58.4 nm) and $\omega_2 = 0.87$ a.u. (52.2 nm). The middle peak is due to the combination of the transition amplitudes via the two paths and their interference at E_{12} . (See figure 1).

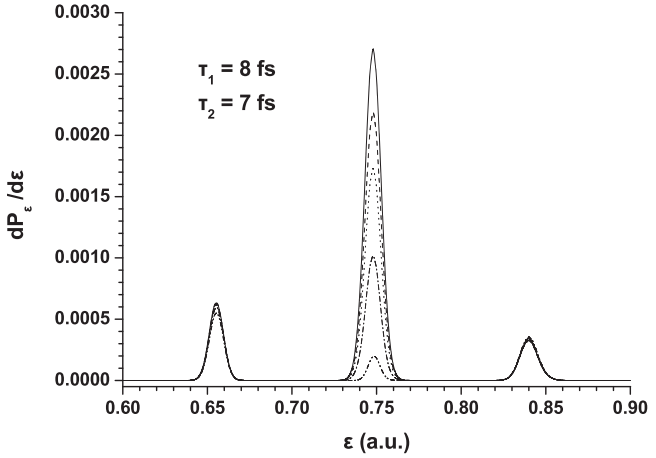

Figure 3. As in figure 2, with τ_1 and τ_2 of the order of 40 cycles of each field. The curves are obtained for negative values of Δt. The solid line curve corresponds to $\Delta t = 0$ fs, the dashed one to $\Delta t = -1.2$ fs, the dotted one to $\Delta t = -2.4$ fs, the dashed–dotted one to $\Delta t = -4.8$ fs, and the dashed–dotted–dotted one to $\Delta t = -24.2$ fs.

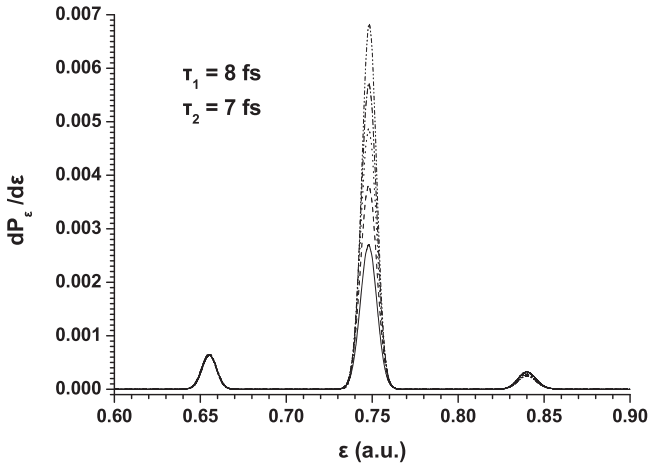

Figure 4. As in figure 3, for positive values of Δt. The solid line curve corresponds to $\Delta t = 0$ fs, the dashed one to $\Delta t = 2.4$ fs, the dotted one to $\Delta t = 4.8$ fs, the dashed–dotted one to $\Delta t = 7.3$ fs, and the dashed–dotted–dotted one to $\Delta t = 16.9$ fs.

rules for linearly polarized light, the level of complexity in dealing numerically with these singularities is reduced significantly.

In accordance with figure 1, the He $1s^2\ ^1S$ state is assumed to interact with two XUV time-delayed pulses. The pulse forms are

$$E(t) = \sum_k E_k(t),$$
$$E_k(t) = F_k e^{-\alpha_k (t-t_k)^2} \cos(\omega_k t),$$
$$k = 1, 2 \qquad (3)$$

$$\alpha_k = \frac{2\ln(2)}{\tau_k^2}, \quad \tau = \text{full width at half-maximum.} \qquad (3a)$$

The time delay is positive or negative, and is defined as

$$\Delta t = t_2 - t_1. \qquad (4)$$

The final results (section 3) determine the photoelectron probability distribution, (per atomic unit of energy)

$$\frac{dP_\varepsilon}{d\varepsilon} = \sum_\ell |\alpha_{\varepsilon,\ell}(T_{end})|^2, \qquad (5)$$

where $\alpha_{\varepsilon,\ell}$ is the coefficient of the energy-normalized state of the continuum at energy ε, with angular momentum ℓ, and T_{end} is the time at which the interaction is essentially zero.

The bulk of the results reported in the paper were obtained for field intensities I_k of the order of 10^{12} W cm^{-2}. They are clear, and demonstrate the physics quantitatively. In particular, the values of F_k (I_k) for which the results presented in figures 2–5 were obtained are

$$F_1 = 0.00534 \text{ a.u.}(I_1 = 1 \times 10^{12} \text{ W cm}^{-2}) \text{and},$$
$$F_2 = 0.015 \text{ a.u.}(I_2 = 8 \times 10^{12} \text{ W cm}^{-2}). \qquad (6)$$

The intensity for the path through the state $1s4p\ ^1P^o$ (52.2 nm), was chosen to be larger because the corresponding dipole matrix element is smaller than the one for $1s^2\ ^1S_0 \rightarrow 1s2p\ ^1P_1^o$ (58.4 nm). Specifically, the excitation matrix elements are, 0.412 a.u. for the $1s^2 - 1s2p$ transition and 0.129 a.u. for the $1s^2$–1s4p transition.

We also carried out SSEA calculations for the higher intensities $I_1 = 1 \times 10^{14}$ W cm^{-2} and $I_2 = 2 \times 10^{14}$ W cm^{-2}. As expected, the field-induced shifts and higher-order state-mixings and interference among multiple transition paths involving discrete and scattering states, are enhanced and cause a blurring of the photoelectron spectrum, which destroys the clear picture for control exhibited by figures 2–5. Such high intensity spectra may have an interest for other types of studies. For the scope of the present application, they served in order to roughly delineate the range of pulse

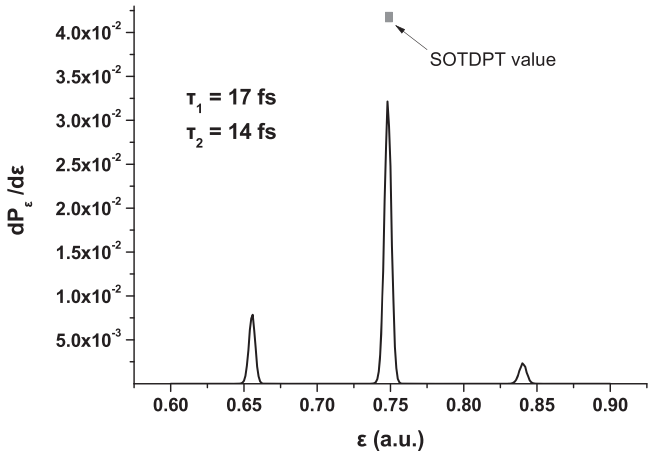

Figure 5. As in figure 2, with τ_1 and τ_2 of the order of 80 cycles of each field. The curves correspond to $\Delta t = 0$. The gray square shows the value calculated from the second order time-dependent perturbation theory (SOTDPT). See text.

parameters for which the spectra are clean, and can be of direct use to future possible experimental investigations.

3. Calculations

The $\Psi(t)$ of equation (1) was calculated at two different levels of theory. In both cases, the relevant *state-specific* electronic structures, electron correlations, and energy-normalized scattering states were taken into account systematically and reliably. The characteristics of the pulses were the same for both levels of theory.

The first level, which is the generally applicable one for problems of time-resolved electron dynamics for strong and/or ultrashort pulses, has to do with the *nonperturbative* calculation of $\Psi(t)$. The SSEA results from this type of solution serve as a reliable reference for both experiment and theory.

Here we note that, because of the simple, closed-shell structure of the Helium ^1S ground state, and because of the simplicity of the one-electron Rydberg character of its $^1P^o$ excited discrete states to which it is connected upon absorption of the first photon, even the '*single-active electron*' (SAE) approximation [15] may produce the phenomenon semi-quantitatively when the intensity is relatively low, of the order 10^{11}–10^{13} W cm^{-2}. However, when the intensity increases, say reaching values of the order of 5×10^{13} W cm^{-2}–1×10^{14} W cm^{-2} and above, then, not only the contributions from the high-energy continuum increase, but also ground state electron correlations and doubly excited states may contribute in higher order. As is well known, the model of the SAE cannot handle electron correlations or double excitations and interchannel couplings.

In either case, (moderate or strong fields), the use of a many-electron theory such as the SSEA guaranties numerical accuracy as well as transparency, and there is no need for discounts in the construction and implementation of the methodology that is generally required for solving the METDSE nonperturbatively.

The second level is that of SOTDPT, where the Gaussian forms of the two pulses and their finite duration of a few femtoseconds were taken into account explicitly.

For the SSEA calculation, the time-dependent wavefunction, $\Psi_{SSEA}(t)$, was constructed and computed in the form

$$\Psi_{SSEA}(t) = \sum_{\ell=0,n=\ell+1} \alpha_{n,\ell}(t)\Phi_n(1s n\ell\ ^1L) + \sum_{\ell=o} \int d\varepsilon \alpha_{\varepsilon,\ell}(t)\Phi_\varepsilon(1s\varepsilon\ell\ ^1L), \quad (7)$$

where Φ_n and Φ_ε are the symmetry-adapted 2-electron bound and energy-normalized scattering wavefunctions for the He states, labeled by each reference configuration.

As explained in [12] and its references, the choice of the N-electron wavefunctions in the SSEA is specific to the electronic structure of each state in the expansion, (discrete, resonance and purely scattering state), and to each problem. The theoretical formulations and methods for their calculation at different levels of approximation, depend on the property/phenomenon of interest. In general, these wavefunctions are constructed from separately optimized *numerical* and *analytic* one-electron functions [16], and its references.

In order to eliminate any numerical inaccuracies and uncertainties, especially when it comes to the diffuse Rydberg wavefunctions, the state-specific bound wavefunctions in expansion (7) were computed and used (in matrix elements) *numerically*, by solving, for each discrete state Φ_n, the multiconfigurational Hartree–Fock (MCHF) or HF (for the Rydberg states) equations, using the code published by Froese-Fischer [17]. The energy-normalized scattering orbitals were obtained numerically in the frozen core of the He^+ 1*s* state.

The ground-state wavefunction, $\Phi(1s^2\ ^1S)$, was obtained from a numerical MCHF calculation with the $1s^2$, $2s^2$, $2p^2$, $3s^2$, $3p^2$, $3d^2$, $4s^2$, $4p^2$, $4d^2$, $4f^2$ configurations, essentially exhausting the relevant to the dynamics contributions of electron correlation. The excited discrete states are of the Rydberg type, $1s n\ell\ ^1L$. They were represented by state-specific numerical HF orbitals with $n = 2,3,4,5,6,7$ and $\ell = 0, 1, 2, 3, 4$, i.e. we included all discrete states up to $1s7g\ ^1G$.

Using energies of the energy-normalized scattering orbitals $\varepsilon\ell$ in the range from 0 to 2.0 a.u. above threshold, and angular momenta with $\ell = 0, 1, 2, 3, 4$, the convergence of the SSEA calculations was very good. The number of coupled equations corresponding to the converged expansion (7) was of the order of 10 000, the overwhelming majority involving, as usual, matrix elements with scattering states.

4. Results from the SSEA and from the time-dependent perturbation theory to second order

Following a series of exploratory SSEA calculations, we identified sets of pulse parameters that can demonstrate with clarity and accuracy the physics of the problem. Specifically, we delineated roughly the region of moderate intensities that

produce photoelectron spectra, (probability distribution per atomic unit of energy), where every peak is interpreted with certainty, (figures 2–5), from the region of strong fields, where the spectrum is altered by being broadened while acquiring additional smaller peaks. One set of moderate intensities which is experimentally practical is given by (6).

We discuss three sets of results, which are presented as figures 2–5. These sets correspond to pulses of about 20, 40 and 80 field-cycles. In order to obtain additional insight, our study also included complementary calculations from the application of SOTDPT.

The formula for the matrix element of the SOTDPT can be found in textbooks, e.g. in chapter 2 of [18]. In the interaction picture, it is formally written as the operator

$$A^{(2)}(t) = (i/\hbar)^2 \int_{-\infty}^{t} dt_1 V_{\rm int}(t_1) \int_{-\infty}^{t_1} dt_2 V_{\rm int}(t_2).$$

Its implementation to the present case of the He middle peak (figure 1) reads

$$\begin{aligned}
&\langle 1sE_{12}\ell\ ^1L^o|A^{(2)}(t)|\ \Phi(1s^2)\rangle \\
&=\left(\frac{-i}{\hbar}\right)^2 \sum_J \int_{-\infty}^{t} dt_1 e^{i(E_{12}-\varepsilon_J)t_1}\langle 1sE_{12}\ell\ ^1L^o|E(t_1)z|\ 1sJp\ ^1P^o\rangle \\
&\quad\times \int_{-\infty}^{t_1} dt_2 e^{i(\varepsilon_J-\varepsilon_{1s^2})t_2}\langle 1sJp\ ^1P^o|E(t_2)z|\ \Phi(1s^2)\rangle \\
&=\left(\frac{-i}{\hbar}\right)^2 \sum_J \langle 1sE_{12}\ell\ ^1L^o|z|\ 1sJp\ ^1P^o\rangle \times \langle 1sJp\ ^1P^o|z|\ \Phi(1s^2)\rangle \\
&\quad\times \int_{-\infty}^{t} dt_1 e^{i(E_{12}-\varepsilon_J)t_1}E(t_1) \times \int_{-\infty}^{t_1} dt_2 e^{i(\varepsilon_J-\varepsilon_{1s^2})t_2}E(t_2),
\end{aligned} \tag{8}$$

where J spans the discrete and the continuous parts of the $^1P^o$ spectrum, and $\ell = s,\ d$.

4.1. Pulses of about 20 field-cycles

The results of the first set with the moderate intensities (6) are displayed in figure 2. They were obtained for τ_k, $k = 1, 2$, of the order of 20 field cycles (duration of about $\tau_1 = 4$ fs and $\tau_2 = 3$ fs). The left and right peaks correspond to the absorption of two ω_1 and two ω_2 photons respectively. These peaks are essentially independent of Δt. A slight dependence is observed when the duration of the pulses is longer- see below.

However, the absorption of one photon from each pulse gives rise, through the combination of the transition amplitudes via the two paths and their interference, (figure 1), to the peak in the middle, whose dependence on Δt is found to be significant: For negative Δt, of the order of 2–5 fs, where the ω_2 pulse precedes the ω_1 pulse, the height of this peak gradually decreases with respect to its value for $\Delta t = 0$. On the contrary, for positive Δt, the height of the peak increases. In the latter case, the upper limit of the ionization probability is determined by the ionization probability of the $1s2p\,^1P^o$ state.

This observable dynamical effect, which was obtained quantitatively from first principles, constitutes the main prediction of this work. Its explanation is as follows:

The choice of the pulse intensities, ($F_2 > F_1$), is such that the Rabi frequencies for both resonant couplings ($1s^2 \xrightarrow{\omega_1} 1s2p$, $1s^2 \xrightarrow{\omega_2} 1s4p$) are essentially the same, which means that the population transfer from $1s^2$ to the two $^1P^o$ states is nearly the same. In the case of (relatively) large negative time delays, i.e. when the pulses do not overlap, the ω_1 pulse starts to act following the fading out of the interaction due to the ω_2 pulse. Hence, the transfer of population from the $1s4p\ ^1P^o$ state to the continuum states $1s\varepsilon s\ ^1S$ and $1s\varepsilon d\ ^1D$ is much weaker than the one resulting when the opposite case holds, namely, when the time delays become positive and large, in which case it is the ω_2 pulse that pumps population from $1s2p\ ^1P^o$ to the continuum. This is so because the dipole transition matrix elements $\langle 1s2p\ ^1P^o|\mathbf{H}_{el}|1s\varepsilon s,\ 1s\varepsilon d\rangle$ are larger than the $\langle 1s4p\ ^1P^o|\mathbf{H}_{el}|1s\varepsilon s,\ \ 1s\varepsilon d\rangle$ ones, and, in addition, the field strengths satisfy $F_2 > F_1$. Therefore, for time delays in the range between (relatively) large negative and large positive values, or, equivalently, in the range between non-overlapping pulses, the height of the middle peak varies continuously.

In addition to the understanding of the phenomenon that is presented in figure 2 in terms of matrix elements and field strengths, it is also of interest to obtain additional quantitative information on how the phenomenon is affected by the states of the full spectrum as a function of the duration (number of field cycles) of the two pulses. We recall that the spectral widths of these pulses are not negligible. For example, for the present case of 20 cycles, these spectral widths are 0.76 eV and 0.62 eV, (depicted on figure 1), when the energy differences between the two $^1P^o$ excited states of interest from their neighboring $^1P^o$ states are, $\Delta E(1s2p,\ 1s3p) = 1.87$ eV, and $\Delta E(1s4p,\ 1s3p) = 0.65$ eV, $\Delta E(1s4p,\ 1s5p) = 0.30$ eV.

For reasons of economy, we considered only the case with $\Delta t = 0$. By comparing the results of the SOTDPT and of the SSEA, the following conclusion is reached: The height of the peak from the SSEA calculation is 2.5×10^{-4}. For the case where J spans the states of the $^1P^o$ discrete spectrum only, then the SOTDPT result is 1.7×10^{-4}. However, when the continuous spectrum is included, the result is essentially the same as that of the SSEA. Hence, we have a quantitative understanding of the significance of the scattering states for these field parameters.

The information concerning the understanding of the participation of the states of the spectrum to the proper description of the middle peak can be gained, in principle, by running a series of SSEA calculations with different expansions, since the structure of the theory allows in a straight forward way to assess the degree of importance of each state-specific wavefunction. However, this is a computationally very time-consuming enterprise. Therefore, we turned to much more economic calculations at the level of SOTDPT, i.e. at the level implied by the scheme (A), where only a subset of the states of the full spectrum is involved. These results were then compared to the SSEA nonperturbative results which are presented in figures 2–5. This comparison sheds light to the understanding of the significance of the contribution to the formation of the middle peak of those states that are not on exact resonance with the center of the two pulses, and of the range of pulse durations and field

Table 1. Analysis of the two-photon transition probabilities in terms of the two paths of scheme and their interference (see equations (8b,c,d)), for the case where the full widths at half maximum, τ_1 and τ_2, are of the order of 40 cycles (see figures 3, 4). They were obtained for negative, (the ω_2 pulse precedes the ω_1 pulse), and positive time delays, given in femtoseconds.

Δt (fs)	P_{1s2p}	P_{1s4p}	$P_{\rm int}$	$P_{\rm tot}$
−24.2	5.21×10^{-11}	2.09×10^{-4}	2.00×10^{-7}	2.09×10^{-4}
−19.4	1.28×10^{-8}	2.09×10^{-4}	3.23×10^{-6}	2.13×10^{-4}
−14.5	1.09×10^{-6}	2.07×10^{-4}	2.97×10^{-5}	2.38×10^{-4}
−9.7	3.33×10^{-5}	1.77×10^{-4}	1.52×10^{-4}	3.63×10^{-4}
−4.8	3.78×10^{-4}	1.29×10^{-4}	4.39×10^{-4}	9.46×10^{-4}
0	1.92×10^{-3}	5.49×10^{-5}	6.36×10^{-4}	2.61×10^{-3}
4.8	4.58×10^{-3}	1.07×10^{-5}	4.39×10^{-4}	5.03×10^{-3}
9.7	6.74×10^{-3}	9.38×10^{-7}	1.58×10^{-4}	6.90×10^{-3}

intensities for which the present problem can be tackled reliably in terms of the SOTDPT.

Numbers from such SOTDPT calculations are contained in table 1, corresponding to the case of 40-cycle pulses—see below. They were obtained in order to discern the degree of contribution to the middle peak of the two paths and of their interference, as a function of the time delay, Δt, ranging from negative to positive values.

4.2. Pulses of about 40 field-cycles

The results of the second set are shown in figures 3 and 4. They were obtained for $\tau_1 = 8$ fs and $\tau_2 = 7$ fs, durations that correspond to about 40 field cycles. The analysis given for the results of figure 2 is also valid for this case. Now, the spectral widths are smaller. They are 0.38 eV and 0.31 eV respectively. Therefore, one should expect that the contribution to the two-photon resonant ionization process of the $1snp\ ^1P^o$ discrete states with $n \neq 2, 4$, as well as of the $1s\varepsilon p\ ^1P^o\ \varepsilon \geqslant 0$ scattering states, should be less important. Indeed, for $\Delta t = 0$, the SSEA value of the height of the middle peak is 2.75×10^{-3}, while the value from equation (8) with J spanning only the discrete $^1P^o$ spectrum is 2.63×10^{-3}. The contribution of the continuous part of the $^1P^o$ spectrum is smaller than before. The total value of the SOTDPT calculation is almost the same as that from the SSEA calculation.

We note that, as figures 2 and 3 for pulses of duration 20 and 40 cycles display, the secondary peaks corresponding to the same-frequency two-photon transitions also show a slight dependence on Δt. This dependence is of no physical relevance to the present predictions. It is due to higher order effects. They are enhanced as the duration of the pulses becomes longer, since the formulas of time-dependent perturbation theory start losing their rigorous validity when, for resonant-ionization transitions, the duration of the pulsed interaction increases. Indeed, this conclusion can be reached quantitatively from calculations which solve such time-dependent problems nonperturbatively, as is the case here.

Finally, using the case of 40 field-cycles, we turn to the quantitative interpretation of the appearance of the middle peak at E_{12}. This is done in terms of the results listed in table 1. From equation (8) and for J corresponding to the intermediate states $1s2p$ and $1s4p$, the two main paths for the process under study can be separated as

$$A_{1sJp}(\ell) = \left(\frac{-i}{\hbar}\right)^2 \int_{-\infty}^{t} dt_1 e^{i(E_{12}-\varepsilon_J)t_1} \langle 1sE_{12}\ell\ ^1L^o|E(t_1)z|\ 1sJp\ ^1P^o\rangle \times \int_{-\infty}^{t_1} dt_2 e^{i(\varepsilon_J-\varepsilon_{1s^2})t_2} \langle 1sJp\ ^1P^o|E(t_2)z|\ \Phi(1s^2)\rangle$$
$$\ell = s,\ d\ \ and\ \ J = 2p,\ 4p. \tag{8a}$$

The probabilities shown in table 1 correspond to the following expressions:

$$(1)\ P_{1s2p} = |A_{1s2p}(\varepsilon s)|^2 + |A_{1s2p}(\varepsilon d)|^2,$$
$$P_{1s4p} = |A_{1s4p}(\varepsilon s)|^2 + |A_{1s4p}(\varepsilon d)|^2 \tag{8b}$$

for the probability involving the paths through the intermediate states $1s2p$ and $1s4p\,^1P^o$,

and

$$(2)\ P_{\rm int} = (A_{1s2p}(\varepsilon s) \times A^*_{1s4p}(\varepsilon s) + \text{c.c.}) + (A_{1s2p}(\varepsilon d) \times A^*_{1s4p}(\varepsilon d) + \text{c.c.}) \tag{8c}$$

for the probability resulting from the interference of the two paths.

The total probability is given by

$$P_{tot} = |A_{1s2p}(\varepsilon s) + A_{1s4p}(\varepsilon s)|^2 + |A_{1s2p}(\varepsilon d) + A_{1s4p}(\varepsilon d)|^2. \tag{8d}$$

It is then possible to distinguish the contribution of each path and of that of their interference to the total probability as a function of time delay Δt.

The numbers in table 1 indicate that for large negative or positive delays, the interference part of the total probability is very small, and so, as expected, each two-photon ionization process evolves essentially independently. On the other hand, for time delays around $\Delta t = 0$, where the two pulses overlap, the process via interference becomes physically significant.

4.3. Pulses of about 80 field-cycles

The results of the third set are shown in figure 5. They were obtained for τ_k, $k = 1, 2$, of about 80 field cycles (duration of about $\tau_1 = 17$ fs, $\tau_2 = 14$ fs), for $\Delta t = 0$. Now, the spectral widths are even smaller, with values 0.19 eV and 0.15 eV

respectively. Yet, a rather significant difference between the SSEA and the SOTDPT results was obtained. In the former case (SSEA), the height of the middle peak is 3.5×10^{-2}, whilst in the latter case (SOTDPT), with J spanning the full $^1P^o$ spectrum, the height is 4.2×10^{-2}. This means that, for the system of interest, the SOTDPT starts to fail for pulses with τ of about 80 field cycles.

This fact is rationalized as follows: The formalism for AC fields corresponding to equation (8), (i.e. $E(t) = \sum_{k=1}^{2} E_k(t) = \sum_{k=1}^{2} F_k \cos(\omega_k t)$, and $E(-\infty) = 0$,—adiabatic switch-on of the fields), shows that the transition amplitude to the middle peak is equal to

$$\langle 1sE_{12}\ell\ ^1L^o|A^{(2)}(\infty)|\ \Phi(1s^2)\rangle = 2\pi\left(\frac{-i}{\hbar}\right)^2\left(\frac{F_1}{2}\right)\left(\frac{F_2}{2}\right)\delta(\varepsilon_{1s^2} - E_{12} + \omega_1 + \omega_2) \times \sum_{k=1,J}^{k=2} \frac{\langle 1sE_{12}\ell\ ^1L^o|z|\ 1sJp\ ^1P^o\rangle\langle 1sJp\ ^1P^o|z|\ \Phi(1s^2)\rangle}{\varepsilon_{1s^2} + \omega_k - \varepsilon_J}. \quad (9)$$

This amplitude diverges when resonant coupling occurs. The derivation of formula (9) from formula (8) is rigorously valid only for AC fields when time is taken to infinity. For very short pulses, each term of the perturbation expansion is small, and, therefore, it is expected that good convergence is quickly obtained. This is a fundamental assumption of perturbation theory for real N-electron systems. As the pulse duration increases, the validity of this assumption is gradually lost. Accordingly, the discrepancy between the nonperturbative SSEA and the SOTDPT results indicates that for pulses with τ_k, $k = 1, 2$, of about 80 field cycles or more, the pulses start approaching rapidly the AC limit. In this limit, the time-dependent perturbation theory to lowest order is inadequate in describing quantitatively, even for moderate intensities, the herein studied two-photon resonant ionization phenomenon.

In view of the results and discussion of the previous subsections, we close with a brief commentary on the Rabi oscillations and their possible effect on the results:

The results that are displayed as figures 2–5, demonstrate the phenomenon as a function of the (positive or negative) *time delay*, Δt, with clarity. In view of the physics of Rabi oscillation, it is useful to see how this is achieved. The field strengths were chosen to be $F_1 = 0.00534$ a.u. and $F_2 = 0.015$ a.u., so as to obtain Rabi frequencies that are almost equal, $\Omega_1 = F_1 < 1s^2|z|1s2p> = 0.0022$ a.u. and $\Omega_2 = F_2 <1s^2|z|1s4p> = 0.002$ a.u. These frequencies correspond to a Rabi cycle of about 70 fs.

A key datum in understanding the degree of significance of Rabi oscillation, is the determination of their number, N_{os}, for pulses that have Gaussian temporal shape. This number can be estimated reliably by using the formula derived in the appendix:

$$N_{os} = F_k V_k \frac{1}{2\sqrt{2\pi\ \ln(2)}}\tau_k\ , \quad k = 1,\ 2, \quad (10)$$

where, $V_1 = \langle 1s^2|z|1s2p\rangle$ *and* $V_2 = \langle 1s^2|z|1s4p\rangle$.

For all cases shown in figures 2–5, the number of Rabi oscillations is much smaller than 1 and therefore, the effects that potentially can arise from them, (e.g. Autler–Townes splitting in the photoionization spectrum), are negligible. This fact explains our choice of this system, (He spectrum plus laser parameters). The aim was to produce results where the control which can be effected by varying Δt, (see the middle peak corresponding to E_{12}), is demonstrable with clarity.

5. Conclusion

Recent developments in experimental research on free-electron laser (FEL) show that it is now possible to produce simultaneously two ultrashort pulses with wavelengths in the XUV range, e.g. [1, 4, 5], Although it appears that problems regarding their consistent characterization persist, (e.g. due to 'jitter'), there is realistic optimism about their systematic use in spectroscopic investigations of time-dependent phenomena associated with electron dynamics.

The theoretical work reported in this paper has proposed and shown computationally with reliable accuracy, that it is possible to use ultrashort *time delays*, Δt, between two XUV pulses of ultrashort duration (about 15 to 80 cycles for wavelengths around 50–60 nm), and of moderate intensities, in order to *control* the dynamics of photoelectron emission based on a scheme that makes good use of different excitation paths leading to the same final state.

Through analysis and trial calculations, we identified excitations in the Helium spectrum, (figure 1), and an appropriate range of pulse parameters, which demonstrate the argument quantitatively in the case of two- XUV photon, (58.4 nm and 52.22 nm), resonant ionization with few-femtosecond Gaussian pulses.

Evidently, if two ultrashort FEL pulses with shorter wavelengths are available for such synchronized interactions, the spectrum must be chosen accordingly. (e.g. larger energy differences in inner-shell resonant excitations or in excitations in the spectra of positive ions).

The predictions and interpretations are quantitative, and are based on the systematic solution of the fundamental equations (1) and (2) nonperturbatively, according to the SSEA [12], as well as perturbatively, according to the results of SOTDPT, equations (8), (9). The relevant results on which the discussion was based, are displayed in figures 2–5 and in table 1.

Appendix

We use the model of a two-state system interacting with a Gaussian pulse in the rotating wave approximation, in order to obtain an analytic expression that connects the full width at half maximum, t_{fwhm}, of the temporal form of intensity, to the number of oscillations between the states. The formula is then applied to the case of He subjected to the Gaussian pulses treated in the text, using the calculated interaction matrix elements, V_1 and V_2.

The time-dependent two-state wavefunction is written as

$$\Psi(t) = b(t)\psi_b + c(t)\psi_c. \tag{A1}$$

Substitution of equation (A1) into the METDSE, and standard algebra that is associated with the two-level model on resonance in the RWA, produce the system of equations

$$\begin{aligned} i\frac{d\beta(t)}{dG(t)} &= \frac{1}{2}VF\gamma(t) \\ i\frac{d\gamma(t)}{dG(t)} &= \frac{1}{2}VF\beta(t). \end{aligned} \tag{A2}$$

Here, $b(t) = e^{-i\varepsilon_b t}\beta(t)$, $c(t) = e^{-i\varepsilon_c t}\gamma(t)$, ε_b and ε_c are the energies of states ψ_b and ψ_c, V is the matrix element of the operator coupling the states, F is the peak field strength, and $G(t)$ is the integral function of the pulse temporal shape $g(t) = \frac{dG(t)}{dt}$.

With the boundary condition $\beta(-\infty) = 1$, the solution of equation (A2) is

$$\beta(t) = \cos\left(\frac{1}{2}FV(G(t) - G(-\infty))\right). \tag{A3}$$

In the case of Gaussian pulse shape, [$g_{Gauss}(t) = e^{-\alpha(t-t_c)^2}$, $\alpha = \frac{2\ln(2)}{t_{fwhm}^2}$], $G(t)$ is given by

$$G(t) = \frac{1}{2}\sqrt{\frac{\pi}{\alpha}}erf(\sqrt{\alpha}(t - t_c)), \tag{A4}$$

where $erf(x)$ is the error function with the known property [19]

$$erf(-\infty) = -1, \quad erf(\infty) = 1. \tag{A5}$$

After some algebra, the time-dependent occupation probability turns out to be

$$|\beta(t)|^2 = \frac{1}{2}\left\{1 + \cos\left(\frac{1}{2}FV\sqrt{\frac{\pi}{2\ln(2)}}t_{fwhm} \times (erf(\sqrt{\alpha}(t - t_c)) - erf(-\infty))\right)\right\}. \tag{A6}$$

It is a modified Rabi oscillation, for which the variation of the argument of the cos() term of (A6) from $t = -\infty$ to $t = +\infty$, is, because of the property (A5)

$$FV\sqrt{\frac{\pi}{2\ln(2)}}t_{fwhm}. \tag{A7}$$

When this quantity is divided by 2π, we obtain the number of oscillations that the two-level system undergoes when subjected to the interaction with the Gaussian pulse:

$$N_{os} = FV\frac{1}{2\sqrt{2\pi\ln(2)}}t_{fwhm}. \tag{A8}$$

ORCID iDs

Theodoros Mercouris https://orcid.org/0000-0001-6073-4039

References

[1] Young L *et al* 2018 Roadmap of ultrafast x-ray atomic and molecular physics *J. Phys. B: At. Mol. Opt. Phys.* **51** 032003

[2] Mercouris T, Komninos Y and Nicolaides C A 2016 EUV two-photon-ionization cross sections of helium from the solution of the time-dependent Schrödinger equation, and comparison with measurements using free-electron lasers *Phys. Rev.* A **94** 063406

[3] Sato T *et al* 2011 Determination of the absolute two-photon ionization cross section of He by an XUV free electron laser *J. Phys. B: At. Mol. Opt. Phys.* **44** 161001

[4] Fushitani M *et al* 2013 Nonresonant EUV-UV two-color two-photon ionization of He studied by single-shot photoelectron spectroscopy *Phys. Rev.* A **88** 063422

[5] Prince K C *et al* 2016 Coherent control with a short-wavelength Free Electron Laser *Nat. Photon.* **10** 176

[6] Shapiro M and Brumer P 2000 Coherent control of atomic, molecular and electronic processes *Adv. At. Mol. Opt. Phys.* **42** 287

[7] Mercouris T and Nicolaides C A 2003 Solution of the many-electron, many-photon problem for strong fields: Application to Li^- in one- and two-color laser fields *Phys. Rev.* A **67** 063403
Mercouris T, Haritos C and Nicolaides C A 2005 Interference generalized cros-section for the multiphoton detachment of in dichromatic fields *J. Phys. B: At. Mol. Opt. Phys.* **38** 399
Mercouris T and Nicolaides C A 2005 Controllable surfaces of path interference in the multiphoton ionization of atoms by a weak trichromatic field *J. Opt. Quantum Semiclass Opt.* **7** S403

[8] Demekhin P, Artemyev A, Kastner A and Baumert T 2018 Photoelectron circular dichroism with two overlapping laser pulses of carrier frequencies and linearly polarized in two mutually orthogonal directions *Phys. Rev. Lett.* **121** 253201

[9] Chen Z, Shapiro M and Brumer P 1994 Interference control of photodissociation branching ratios. Two-color frequency tuning of intense laser fields *Chem. Phys. Lett.* **228** 289

[10] Pratt S T 1996 Interference effects in the two-photon ionization of nitric oxide *J. Chem. Phys.* **104** 5776

[11] Wang F and Elliott D S 1997 Product-state control through interfering two-photon ionization routes *Phys. Rev.* A **56** 3065

[12] Mercouris T, Komninos Y and Nicolaides C A 2010 The state-specific expansion approach to the solution of the polyelectronic time-dependent Schrödinger equation for atoms and molecules in unstable states *Adv. Quantum Chem.* **60** 333

[13] Loudon R 1983 *The Quantum Theory of Light* 2nd edn (Oxford: Clarendon)

[14] Komninos Y, Mercouris T and Nicolaides C A 2017 Theory and computation of electromagnetic transition matrix elements in the continuous spectrum of atoms *Eur. Phys. J.* D **71** 8

[15] Kulander K C 1988 Time-dependent theory of multiphoton ionization of Xenon *Phys. Rev.* A **38** 778

[16] Nicolaides C A 2017 Resonances in the continuum, field-induced nonstationary states, and the state-and property-specific treatment of the many-electron problem *Adv. Quantum Chem.* **74** 149

[17] Froese-Fischer C 1978 A general multi-configuration Hartree–Fock program *Comput. Phys. Commun.* **14** 145

[18] Faisal F H M 1987 *Theory of Multiphoton Processes* (New York: Plenum Press)

[19] Abramowitz M and Stegun I A 1972 *Handbook of Mathematical Functions* (New York: Dover)